



**OPEN** **A critical role for IL-21/IL-21 receptor signaling in isoproterenol-induced cardiac remodeling**

Bing Qi<sup>1,2</sup>, Ruohang Xu<sup>1,2</sup>, Yanye Jin<sup>1,2</sup>, Yufei Wang<sup>1,2</sup>, Tianwei Cheng<sup>1,2</sup>, Chang Liu<sup>1,2</sup>, Yujin Ji<sup>1,2</sup>, Lihong Guo<sup>3</sup>, Jing Li<sup>1,2</sup>, Yang Gao<sup>1,2</sup>, Yang Xu<sup>1,2</sup>, Jianlin Cui<sup>1,2</sup>, Jie Liu<sup>1,2</sup>, Zecheng Jiang<sup>4</sup>✉, Lifeng Feng<sup>1,2</sup>✉, Zhi Qi<sup>1,2,3,5,6</sup>✉ & Liang Yang<sup>1,2</sup>✉

Increased cytokine secretion from immune cells is often associated with cardiac remodeling and heart failure due to pressure overload. Several reports suggest that the IL-21/IL-21 receptor (IL-21R) signaling pathway may play a critical role in heart failure progression, but the exact mechanism remains unclear. In this study, isoproterenol (ISO) was used to induce heart failure in mice and found that ISO injection caused significant upregulation of IL-21 and the IL-21R in the heart of mice. Subsequently, IL-21 receptor-deficient ( $\text{IL-21R}^{-/-}$ ) mice were used to evaluate the cardioprotective effects of IL-21/IL-21R. Importantly, we found a significant reduction in myocardial hypertrophy, inflammation, and apoptosis in ISO-treated  $\text{IL-21R}^{-/-}$  mice compared to WT mice. Furthermore, the frequency of  $\text{CD4}^+ \text{IFN-}\gamma^+$  cells was significantly reduced in ISO-treated  $\text{IL-21R}^{-/-}$  mice. Co-culture studies showed that the adhesion rate of  $\text{CD4}^+ \text{T}$  cells isolated from  $\text{IL-21R}^{-/-}$  to cardiac fibroblasts was significantly reduced compared to co-cultures isolated from WT mice. Accordingly, significant downregulation of  $\alpha\text{-SMA}$  was detected in cardiac fibroblasts when cocultured with  $\text{CD4}^+ \text{T}$  cells isolated from  $\text{IL-21R}^{-/-}$  mice. Furthermore, IL-21 could directly induce cardiomyocyte hypertrophy and apoptosis and exacerbate ISO-induced myocardial damage through activation of STAT3 signaling pathway. Our study demonstrates the mechanism of IL-21 and its receptor in the progression of myocardial hypertrophy and fibrosis and highlights that the absence of IL-21R may provide protection against myocardial damage, thus providing a new potential therapeutic target for the treatment of heart failure.

**Keywords** Cardiac hypertrophy, IL-21, STAT3

Heart failure (HF) is a major public health problem worldwide, affecting more than 26 million people, and its prevalence continues to increase as the population ages and chronic diseases increase<sup>1,2</sup>. Cardiac remodeling, characterized by cardiac hypertrophy and myocardial fibrosis, is the basis for the occurrence and development of heart failure<sup>3,4</sup>. Numerous pathophysiological mechanisms are involved in cardiac remodeling, including neurohormonal activation, inflammation, oxidative stress, and changes in extracellular matrix composition, leading to cardiac hypertrophy and fibrosis<sup>5,6</sup>. Furthermore, there is increasing recognition of the role that immune system activation plays in the development and progression of cardiac remodeling and heart failure.

Interleukin-21 (IL-21) is a class I cytokine member secreted primarily by activated  $\text{CD4}^+ \text{T}$  cells and natural killer T cells<sup>7,8</sup>. It exerts widespread immunomodulatory effects and is involved in the pathogenesis of autoimmune diseases, viral infections, and several types of cancers<sup>9,10</sup>. IL-21 signals through a heterodimeric receptor complex consisting of its unique receptor IL-21R and the common receptor  $\gamma$ -chain<sup>11</sup>. The IL-21R is commonly expressed by immune cells, such as T cells, B cells, macrophages and neutrophils<sup>12</sup>. Recently, expression of IL-21R was also detected in non-immune cells, including fibroblasts, endothelial cells and neurons, suggesting the possibility that IL-21/IL-21R could modulate additional inflammatory pathways in addition to its regulatory effects on cellular immunity<sup>13</sup>. Recently, high serum IL-21 level was reported to be an independent predictor of LV remodeling in post-MI patients<sup>14</sup>. Other reports reveal that IL-21 stimulates myocardial

<sup>1</sup>Department of Molecular Pharmacology, School of Medicine, Nankai University, Tianjin 300071, China. <sup>2</sup>Core Laboratory, Beichen Hospital, Nankai University, Tianjin 300071, China. <sup>3</sup>Institute of Digestive Disease, Shengli Oilfield Central Hospital, Dongying 257000, China. <sup>4</sup>Department of Biology, Temple University, Philadelphia, PA 19122, USA. <sup>5</sup>Tianjin Key Laboratory of General Surgery in Construction, Tianjin Union Medical Center, Tianjin 300122, China. <sup>6</sup>The First Department of Critical Care Medicine, The First Affiliated Hospital of Shihezi University, Shihezi 832003, China. ✉email: zecheng.jiang@temple.edu; 9820220108@nankai.edu.cn; qizhi@nankai.edu.cn; yangliang@nankai.edu.cn

inflammation and fibrosis through activation of the TIMP4/MMP9 signaling pathway, ultimately leading to myocardial remodeling in response to stress overload<sup>15</sup>. However, the role of IL-12/IL21R in isoproterenol-induced cardiac remodeling and heart failure development remains to be further elucidated.

In the present study, we found that both IL-21 and IL-21R levels were significantly upregulated after isoproterenol injection. Knocking down IL-21R protects against myocardial damage and reduces ISO-induced apoptosis in mice. Furthermore, knockout of IL-21R led to a reduction in IFN- $\gamma$ -producing Th1 cells and reduced adhesion to cardiac fibroblasts in vitro, leading to an improvement in ISO-induced myocardial fibrosis. Furthermore, IL-21 directly promotes cardiomyocyte hypertrophy and apoptosis in vitro. The potential signaling mechanisms underlying these responses may involve STAT3 signaling pathways.

## Results

### IL-21 and IL-21R expression increased in hypertrophic myocardium induced by ISO injection

To assess the role of IL-21/IL-21R in hypertrophic myocardium, we simulated a mouse model of myocardial hypertrophy by subcutaneous injection of isoproterenol. As shown in Fig. 1A, compared to the control group, the heart weight/body weight (HW/BW) and heart weight/tibia length (HW/TL) ratios were significantly increased in mice after 7 days of ISO treatment. The WGA results showed an increase in myocardial surface area in the ISO-treated group (Fig. S1A). Furthermore, qPCR analysis showed upregulation of IL-21 and IL-21R, consistent with an increase in hypertrophy markers ANF in cardiac tissue after ISO injection on days 3 and 7 (Fig. 1B). Likewise, western blot results showed that the protein expression of IL-21, IL-21R and ANF were significantly increased after 7 days of ISO injection (Fig. 1C,D). Next, immunofluorescence staining was performed to determine the location of IL-21R in cardiomyocytes, which indicated that IL-21R was mainly distributed on the cell membrane of myocardial cells (Fig. 1E,F). Quantification of immunofluorescence experiments also showed that the levels of IL-21 and its receptor were significantly increased after ISO injection (Fig. S1C,D). To further clarify the origin of IL-21 expressing cells, we then used intracellular cytokine staining in combination with staining of some surface markers. Analysis of immune cells from the mediastinal lymph nodes revealed an increase in CD4 $^{+}$ IL-21 $^{+}$  cells in the ISO treatment group (Fig. 1G), while there was no difference Ly-6C $^{+}$ IL-21 $^{+}$  and Ly-6G $^{+}$ IL-21 $^{+}$  cells compared to the control group (Fig. S1E,F), indicating that CD4 $^{+}$  cells were the main source of IL-21. These data suggest that ISO stimulation can trigger activation of IL-21 signaling in the myocardium.

### IL-21R knockout alleviates ISO-induced cardiac hypertrophy and apoptosis

To assess the role of IL-21R in cardiac function, IL-21R $^{-/-}$  mice were used and echocardiographic analysis was performed after isoproterenol injection. ISO injection led to cardiac dysfunction in WT mice, as evidenced by a decrease in left ventricular ejection fraction (EF) and fractional shortening (FS), while cardiac contractile function was preserved in IL-21R $^{-/-}$  mice (Fig. 2A,D). In addition, the H/W and H/T were higher in ISO-treated WT mice than in control WT mice, while these ratios were restored in IL-21R $^{-/-}$  mice after ISO treatment (Fig. S2A). The results of WGA staining showed a significant increase in the cross-sectional area of cardiomyocytes in ISO-treated WT mice, while this hypertrophic effect was reduced in IL-21R $^{-/-}$  mice (Fig. 2B,E). TUNEL results indicate that the percentage of apoptotic myocardial nuclei was significantly higher in WT hearts than IL-21R $^{-/-}$  hearts in the ISO-treated group (Fig. 2C,F). Furthermore, qPCR results showed that ISO treatment increased the mRNA expression levels of ANF, BNP, BAX, and Bcl-2 in WT mice, while IL-21R knockout significantly decreased the expression levels of hypertrophy-related genes (ANE, BNP) and apoptosis markers (BAX, Bcl-2) (Fig. S2B). Western blot analysis also confirmed that the expression of ANF and BAX in ISO-treated WT hearts was significantly higher than that in IL-21R $^{-/-}$  hearts (Fig. 2G,H). This suggests that IL-21R knockout protects against ISO-induced cardiac dysfunction and myocardial injury.

### IL-21R knockout ameliorated ISO-induced cardiac fibrosis in mice

After ISO treatment, the extent of myocardial fibrosis was assessed using HE, Masson and Picosirius red staining. There was no significant difference in the extents of myocardial fibrosis in WT and IL-21R $^{-/-}$  mice in the sham groups. However, the HE staining results showed significant tissue damage and structural disarray in the myocardial tissue of WT mice following ISO treatment, whereas the IL-21R $^{-/-}$  mice did not exhibit such damage (Fig. 3A). Masson staining (Fig. 3B) and Picosirius red staining (Fig. 3C) also showed a significant increase in fibrosis in ISO-treated WT mice, whereas fibrosis was reduced in IL-21R $^{-/-}$  mice (Fig. 3D,E). Consistent with the data of quantitative analysis of fibrosis in myocardial sections, qPCR results showed that the expression levels of TGF- $\beta$ ,  $\alpha$ -SMA, Fn1, collagen I, collagen III, and collagen IV mRNAs were up-regulated in ISO-injected WT cardiac tissue samples, whereas the expression of these genes was decreased in ISO-treated IL-21R $^{-/-}$  hearts (Fig. 3F,G). These analyses further support that IL-21R knockout effectively alleviates ISO-induced myocardial fibrosis.

### IL-21R knockout mice exhibited reduced Th1 responses after ISO injection

T cells can influence cardiac fibroblasts (CFBs) to promote cardiac fibrosis in non-ischemic heart failure (HF)<sup>16</sup>. Therefore, we next investigated whether IL-21 signaling could affect the degree of fibrosis by regulating T cell function. As shown in Fig. 4A, a significant increase of mRNA levels of STAT4, T-bet, and IFN- $\gamma$ , the signature cytokine and transcription factor for Th1 cells, was observed in ISO-treated WT mice. In contrast, STAT4, T-bet, and IFN- $\gamma$  mRNA levels were decreased in ISO-treated IL-21R $^{-/-}$  mice. Flow cytometry analysis revealed similar results, showing an increase in CD4 $^{+}$ IFN- $\gamma$  $^{+}$  cells in the mLNs of ISO-treated WT mice, which was not observed in ISO-treated IL-21R $^{-/-}$  mice (Fig. 4B,C). Next, to further validate the role of Th1 cells in myocardial fibrosis, we isolated CD4 $^{+}$  T cells from the mediastinal lymph nodes (mLN) of WT, IL-21R $^{-/-}$ , and ISO-treated WT and IL-21R $^{-/-}$  mice and co-cultured them with primary cardiac fibroblasts (CFBs). The results showed that, compared to control mice, CD4 $^{+}$  T cells from ISO-treated WT mice adhered more firmly to CFBs, whereas CD4 $^{+}$

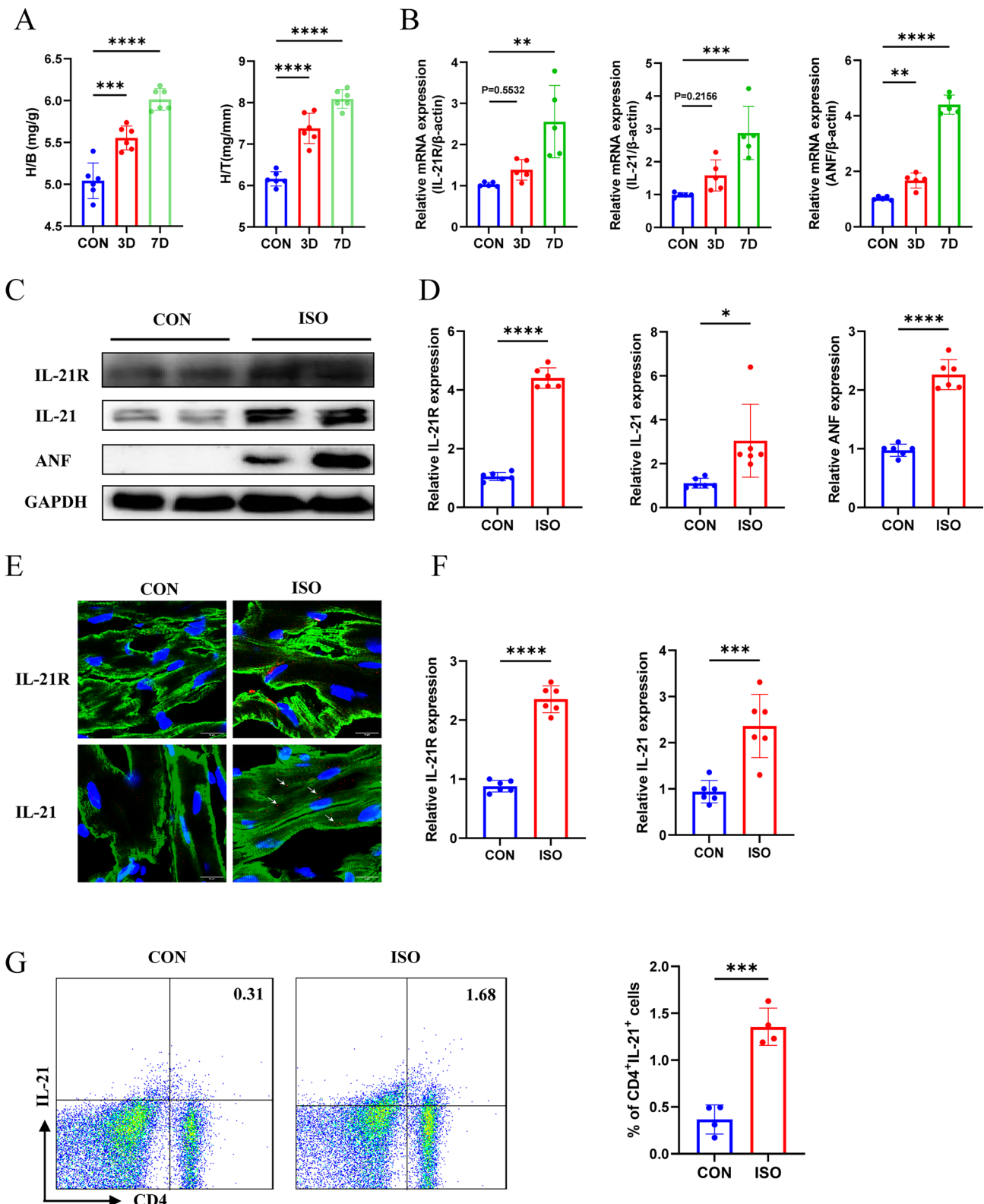


**Fig. 1.** Increased expression of IL-21/IL-21R in hypertrophic myocardium in mice. (A) Heart weight/tibia length (H/T) and heart weight/body weight (H/B) were calculated. n=6. (B) Relative quantification of IL-21R, IL-21, and ANF mRNA levels in cardiac tissue after subcutaneous injection of isoprenaline in mice for 3 and 7 days, n=5. (C,D) Western blot analysis of IL-21R, IL-21 and ANF in myocardial tissue and their quantification, n=6. (E,F) Representative immunofluorescence images showing IL-21R and IL-21 expression. IL-21-positive areas are indicated by white arrows; scale bar: 10 μm. n=6. (G) Flow cytometry analysis of lymphocytes in mediastinal lymph nodes (mLNs) and their quantification, n=5. Figure 1 was created using Adobe Illustrator 2025. Data are presented as mean ± SEM. \*p<0.05, \*\*p<0.01, \*\*\*p<0.001, \*\*\*\*p<0.0001.

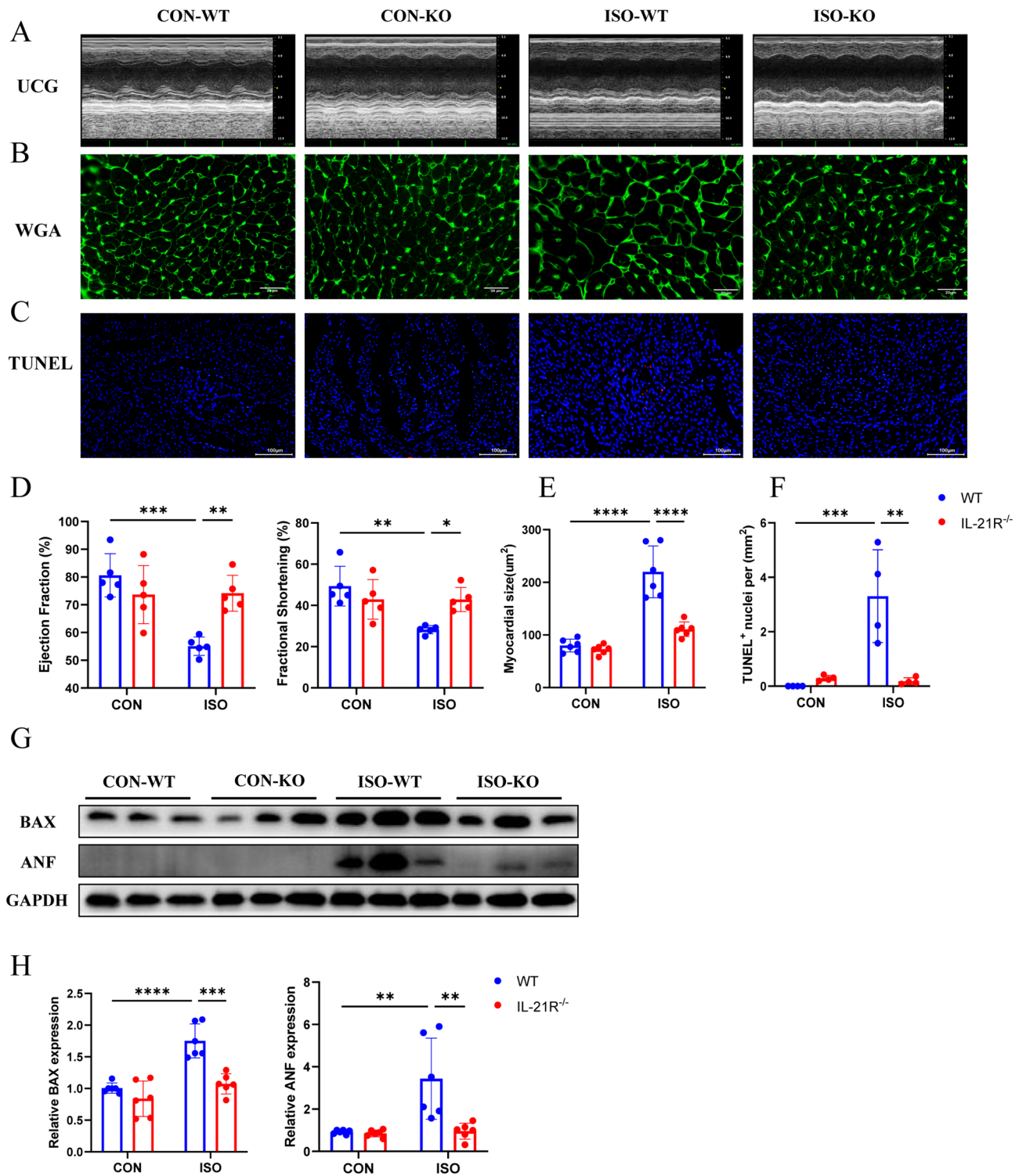


**Fig. 2.** Knockout of the IL-21R reduces cardiac hypertrophy and apoptosis caused by ISO. (A) Representative echocardiograms for each group after ISO subcutaneous injection. (B) Representative WGA staining images, scale bar: 20  $\mu$ m. (C) Representative TUNEL staining images, scale bar: 100  $\mu$ m. (D) Quantification of ejection fraction (EF) and fractional shortening (FS) for each group, n = 5. (E) Quantification of WGA staining, n = 6. (F) Quantification of TUNEL staining, n = 4. (G,H) Western blot analysis of ANF and BAX in myocardial tissue and their quantification, n = 6. Data are presented as mean  $\pm$  SEM. \*p < 0.05, \*\*p < 0.01, \*\*\*p < 0.001, \*\*\*\*p < 0.0001.

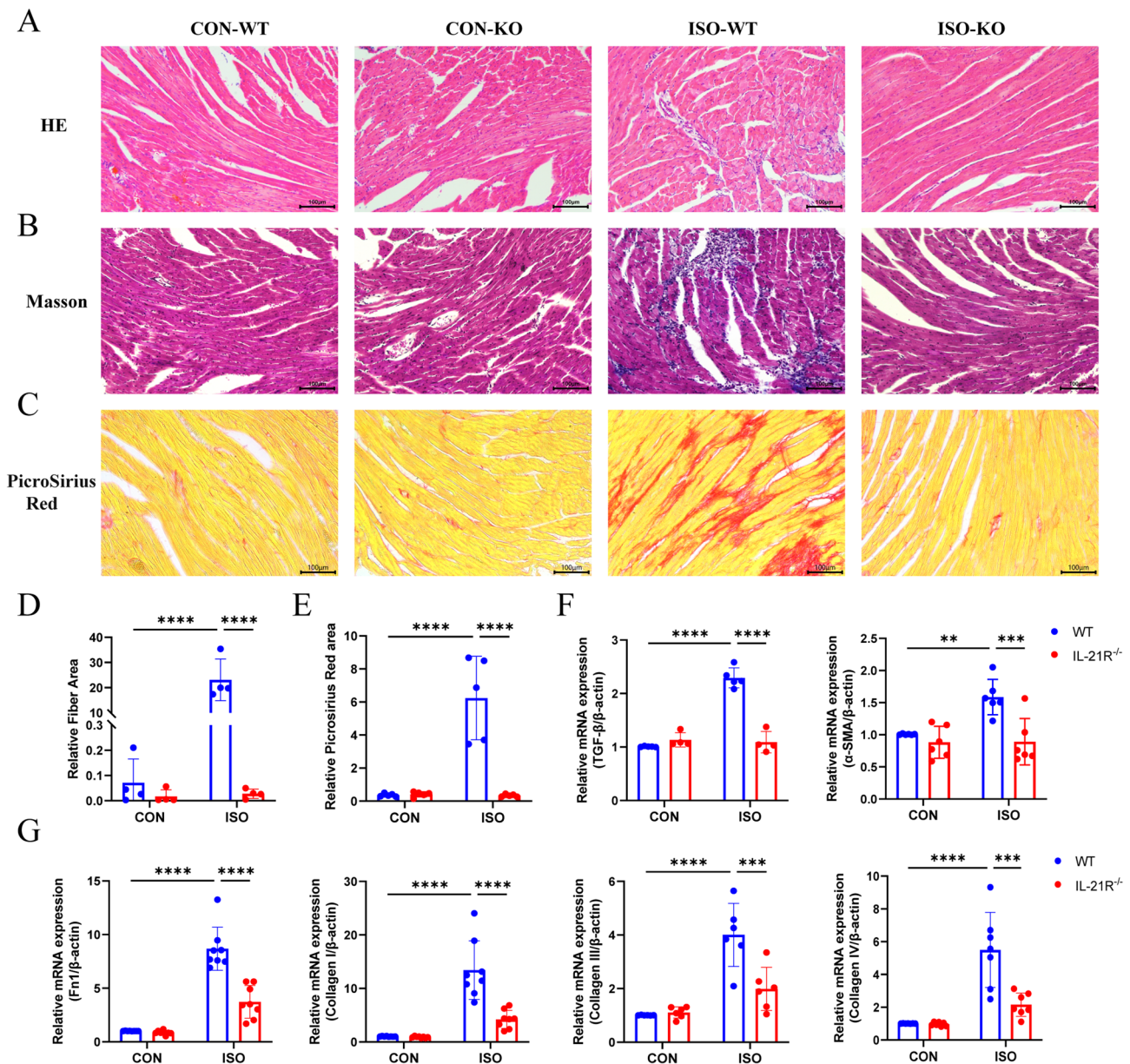
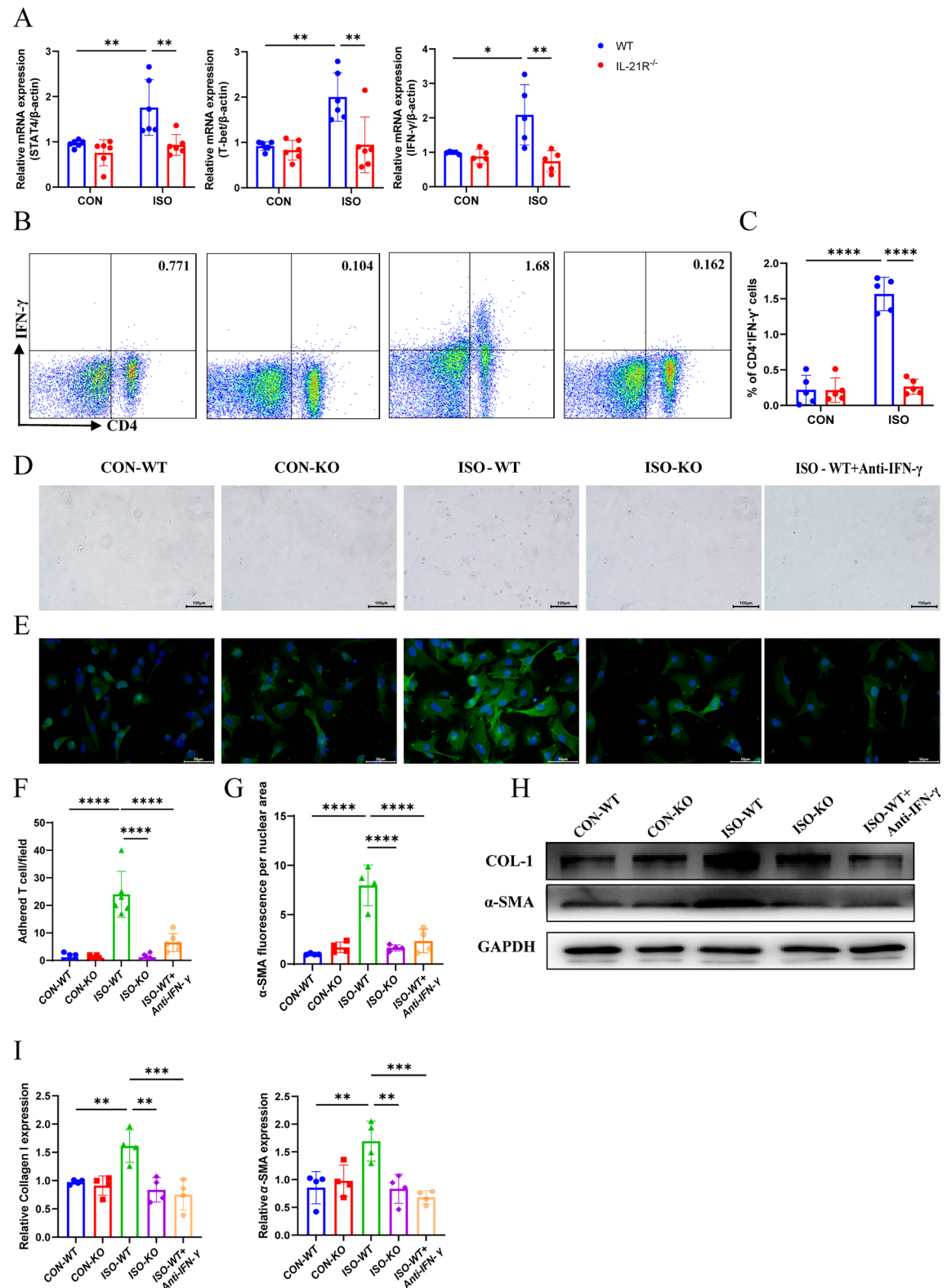


**Fig. 3.** Knocking out the IL-21R improved ISO-induced cardiac fibrosis in mice. (A) Representative hematoxylin and eosin (HE) staining images, scale bar: 100  $\mu$ m. (B) Representative Masson staining images, scale bar: 100  $\mu$ m. (C) Representative Picosirius Red staining images, scale bar: 100  $\mu$ m. (D) Quantification of Masson trichrome staining, n = 4. (E) Quantification of Picosirius Red staining, n = 5. (F,G) Relative quantification of mRNA levels of TGF- $\beta$  (n = 5),  $\alpha$ -SMA (n = 6), Fn1 (n = 8), Collagen I (n = 8), Collagen III (n = 6), and Collagen IV (n = 7) in myocardial tissue. Data are presented as mean  $\pm$  SEM. \*p < 0.05, \*\*p < 0.01, \*\*\*p < 0.001, \*\*\*\*p < 0.0001.

T cells from IL-21R<sup>-/-</sup> mice exhibited significantly reduced adhesion to CFBs (Fig. 4D,F). Immunofluorescence staining analysis revealed that, compared to CFBs co-cultured with CD4<sup>+</sup> T cells from ISO-treated WT mice, CFBs co-cultured with CD4<sup>+</sup> T cells from ISO-treated IL-21R<sup>-/-</sup> mice exhibited significantly lower expression of the myofibroblast marker  $\alpha$ -SMA (Fig. 4E,G). Furthermore, the addition of an IFN- $\gamma$  antibody effectively reduced CD4<sup>+</sup> T cell adhesion to CFBs and suppressed  $\alpha$ -SMA expression in CFBs. Western blot analysis further confirmed that, compared to the control group, the expression of collagen I and  $\alpha$ -SMA was significantly upregulated in CFBs co-cultured with CD4<sup>+</sup> T cells from ISO-treated WT mice, whereas their expression levels were lower in CFBs co-cultured with CD4<sup>+</sup> T cells from ISO-treated IL-21R<sup>-/-</sup> mice. Additionally, in the CFBs co-cultured with CD4<sup>+</sup> T cells from ISO-treated WT mice, the expression of collagen I and  $\alpha$ -SMA decreased significantly after addition of IFN- $\gamma$  antibody, resulting in a pattern similar to that observed in the ISO-treated IL-21R<sup>-/-</sup> mice (Fig. 4H,I). These results were consistent with the findings from immunofluorescence staining. All these results suggest that CD4<sup>+</sup> T cells activated in the mLNs and expressing mainly IFN- $\gamma$  in the setting



of ISO-induced heart failure adhere to CFB and induce CFB transition to profibrotic myofibroblasts, IL-21R deficiency may affect CFB conversion to myofibers by reducing the adhesion of IFN- $\gamma$  producing Th1 cells to CFB.

### IL-21 promotes cardiomyocyte hypertrophy and apoptosis

To further validate the role of IL-21 signaling in the myocardium at the cellular level, primary mouse cardiomyocytes were treated with recombinant IL-21 protein and analyzed after 24 h. The mRNA results showed that IL-21-treated cardiomyocytes had increased expression of ANF and BNP, the genes associated with myocardial hypertrophy, compared to the control group. Interestingly, we found that IL-21R expression was

**Fig. 4.** Mice lacking the IL-21R showed diminished Th1 responses following ISO injection. (A) Relative quantification of STAT4 ( $n=6$ ), T-bet ( $n=6$ ), and IFN- $\gamma$  ( $n=5$ ) mRNA levels in mLNs. (B,C) Flow cytometry analysis of mLNs and its quantification,  $n=5$ . (D) CD4 $^{+}$  T cells were isolated from the mediastinal lymph nodes (mLNs) of control, ISO-treated WT, and ISO-treated IL-21R $^{-/-}$  mice. Another group consisted of CD4 $^{+}$  T cells from ISO-treated WT mice co-cultured with CFBs in the presence of exogenous IFN- $\gamma$  antibody (0.5  $\mu$ g/ml). After 24 h of co-culture, adherent CD4 $^{+}$  T cells on CFBs were imaged. Cells were co-cultured at a 5:1 ratio (CFB/T cells) and photographed after washing, scale bar: 100  $\mu$ m. (E) Immunofluorescence analysis of  $\alpha$ -SMA in CFBs after 24-h co-culture with CD4 $^{+}$  T cells from control or ISO-treated WT and IL-21R $^{-/-}$  mice, scale bar: 50  $\mu$ m. (F) Quantification of CD4 $^{+}$  T cells adhered to CFBs,  $n=6$ . (G) Quantification of  $\alpha$ -SMA immunofluorescence staining,  $n=4$ . (H–I) Western blot analysis of  $\alpha$ -SMA and Collagen I expression in CFBs after 24 h co-culture and its quantification,  $n=3$ . Data are presented as mean  $\pm$  SEM. \* $p<0.05$ , \*\* $p<0.01$ , \*\*\* $p<0.001$ , \*\*\*\* $p<0.0001$ .

also upregulated by IL-21 incubation (Fig. 5A). To verify whether IL-21 has an influence on cardiomyocyte hypertrophy, we observed that IL-21 treatment significantly increased the area of primary mouse cardiomyocytes, further confirming the notion that IL-21 induces cardiomyocyte hypertrophy (Fig. 5B,D). We next examined the influence of IL-21 on cardiomyocyte apoptosis. Immunofluorescence staining showed a significant increase in the number of TUNEL-positive cells in the IL-21-treated group, suggesting that IL-21 treatment induced greater cardiomyocyte apoptosis (Fig. 5C,E). Western blot analysis showed that IL-21 upregulated the expression of the hypertrophy marker ANF and the pro-apoptotic protein BAX (Fig. 5F,G). These results suggest that IL-21 can promote cardiomyocyte hypertrophy and apoptosis.

### IL-21 regulates cardiomyocyte hypertrophy and apoptosis via the STAT3 pathway

Previous studies have shown that IL-21-mediated cellular effects can be regulated through various signaling pathways, such as JAK-STAT, PI3K, and MAPK pathways, with STAT3 playing a major role in the biological actions of IL-21<sup>17</sup>. To further elucidate the mechanisms by which IL-21 affects cardiomyocyte hypertrophy, we focused on these signaling pathways. As shown in Fig. 6A, western blot analysis showed increased phosphorylation of p-STAT3 in ISO-treated WT hearts, while p-STAT3 phosphorylation was reduced in IL-21R $^{-/-}$  hearts after 7 days of ISO injection. Then, we assessed the activation kinetics of the STAT3 signaling pathways at a cellular level. We found that STAT3 phosphorylation was enhanced by IL-21 administration at early time points (30 min) and returned to baseline after 3 h. Furthermore, we found that the P-ERK signaling pathway was activated, with P-ERK activation peaking at 1 h and returning to baseline at 6 h (Fig. 6B). To further demonstrate that IL-21 causes myocardial hypertrophy and apoptosis via the STAT3 signaling pathway, we next stimulated primary mouse cardiomyocytes with IL-21 for 24 h in the presence and absence of WP1006 (STAT3 phosphorylation inhibitor). Real-time PCR results showed that, the upregulation of ANF, BNP, and BAX and the downregulation of Bcl-2 in primary mouse cardiomyocytes induced by IL-21, were all reversed in the presence of WP-1006 (Fig. S4A). The results of TUNEL staining and phalloidin staining indicate that the IL-21-induced increase in cell area and apoptosis could be inhibited by WP-1066 (Fig. 6C,D). Western blotting also showed that pretreatment with WP-1006 could reduce IL-21 incubation-induced phosphorylation of STAT3, expression of hypertrophic markers (ANF) and pro-apoptotic proteins (BAX) (Fig. 6E). This finding supports the notion that IL-21 promotes myocardial apoptosis and hypertrophy through activation of the STAT3 signaling pathway.

### Discussion

The results of the present study indicate that IL-21 is a key factor in the induction of myocardial injury during heart failure. After myocardial injury, IL-21 accumulates in the mouse heart, and knockdown of the IL-21R significantly attenuated ISO-induced cardiomyocyte inflammation and apoptosis. ISO-induced myocardial injury was also accompanied by a significant increase in the adhesion of T cells to cardiac fibroblasts, which led to an increase in the degree of fibrosis. IL-21 induces myocyte hypertrophy and apoptosis through the modulation of the P-STAT3/STAT3 signaling pathway. And apoptosis by regulating the P-STAT3/STAT3 signaling pathway. These data reveal the complex role of IL-21 in inducing myocardial injury during heart failure.

Interleukin-21 (IL-21) is a critical immunomodulatory cytokine primarily secreted by activated CD4 $^{+}$  T cells and natural killer (NK) cells. Its receptor, IL-21R, is widely expressed on various immune and non-immune cells, including cardiomyocytes<sup>10,12</sup>. In recent years, an increasing number of studies have revealed the potential roles of IL-21 and IL-21R in cardiac health and disease<sup>18</sup>. Although IL-21R expression in cardiac tissue is generally low, its levels are significantly elevated in certain cardiac disease states<sup>19</sup>. These findings are consistent with our experimental results, where we observed upregulation of both IL-21R and IL-21 in ISO-induced myocardial injury. This suggests that the IL-21/IL-21R signaling pathway may play a critical role in regulating cardiac function.

To investigate the role of the IL-21 signaling pathway in the progression of heart failure, we utilized IL-21R knockout mice. Recent studies have shown that excessive activation of the IL-21 signaling pathway can lead to heightened inflammation, exacerbating cardiac injury and promoting myocardial fibrosis, ultimately worsening cardiac function<sup>20,21</sup>. Additionally, overexpression of IL-21 can cause a significant influx of inflammatory cells into cardiac tissue, and this sustained inflammatory response not only damages cardiomyocytes but may also trigger chronic heart failure<sup>22,23</sup>. In the myocardium of ISO-treated mice, we observed significant improvement in cardiac function, along with reduced myocardial hypertrophy, fibrosis, and apoptosis in IL-21R $^{-/-}$  mice compared to WT mice (Fig. 2). On one hand, IL-21 plays a critical role in regulating immune cells, such as

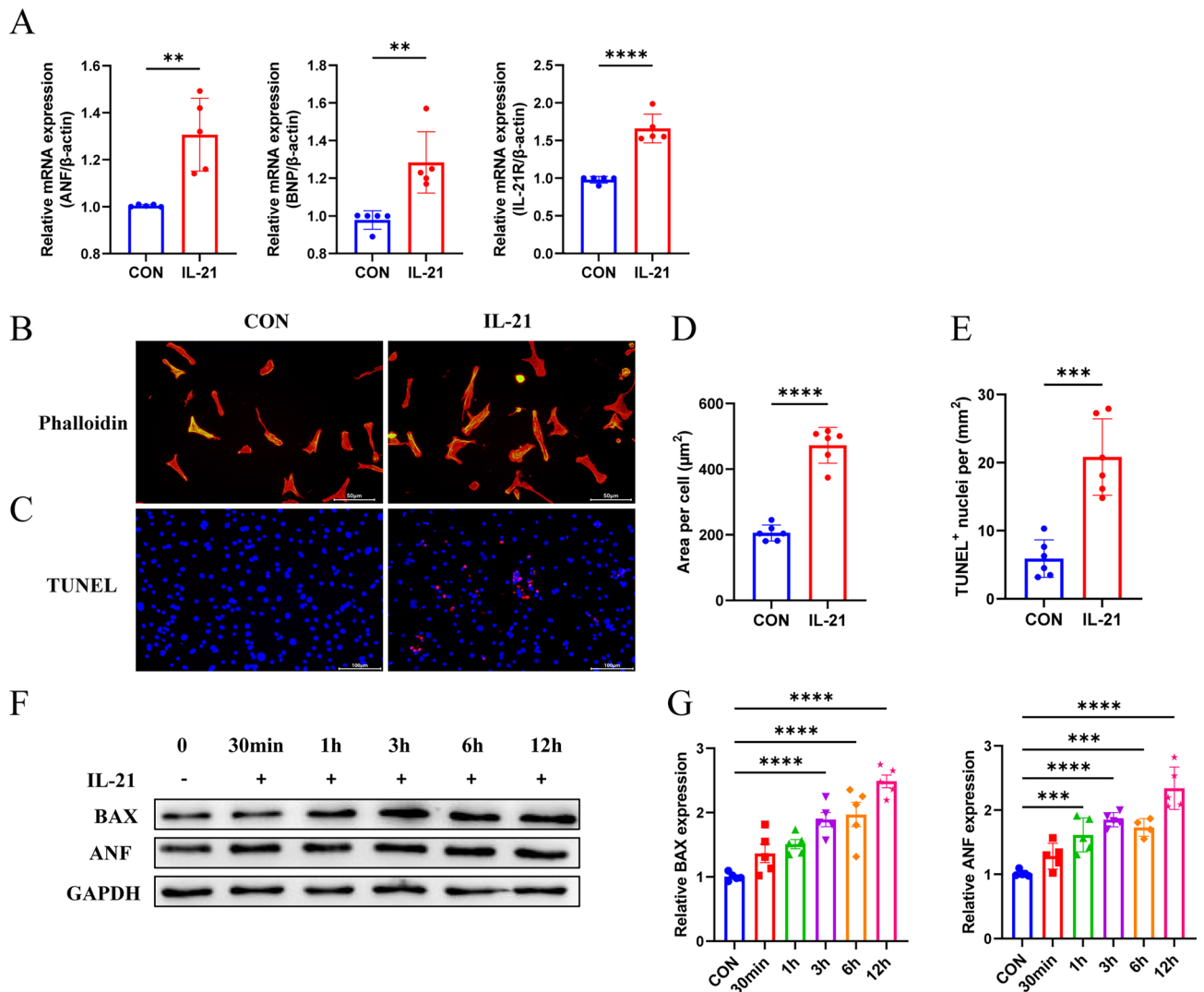


**Fig. 5.** IL-21 induces hypertrophy and apoptosis in cardiomyocytes. Primary mouse cardiomyocytes were treated with IL-21 (100 ng/ml) for subsequent analyses. (A) Relative quantification of IL-21R, ANF, and BNP mRNA levels in primary mouse cardiomyocytes, n=5. (B) Representative phalloidin staining of primary cardiomyocytes, scale bar: 50  $\mu\text{m}$ . (C) Representative TUNEL staining of primary cardiomyocytes, scale bar: 100  $\mu\text{m}$ . (D) Quantification of cell area after phalloidin staining, n=6. (E) Quantification of TUNEL staining, n=6. (F,G) Western blot analysis of, ANF, and BAX expression in primary mouse cardiomyocytes after IL-21 treatment for different durations, and their quantification, n=5. Data are presented as mean  $\pm$  SEM. \*p<0.05, \*\*p<0.01, \*\*\*p<0.001, \*\*\*\*p<0.0001.

T cells and B cells, enhancing the host's resistance to pathogens and helping prevent further cardiac damage caused by infections<sup>24,25</sup>. However, in some cases, dysregulation of the IL-21-mediated immune response may be closely linked to the progression of heart disease<sup>26</sup>. We observed an increase in CD4<sup>+</sup>IL-21<sup>+</sup> expression in the myocardium of ISO-treated mice (Fig. 1G), along with a rise in IFN- $\gamma$ <sup>+</sup>CD4<sup>+</sup> expression (Fig. 4B). These heightened immune responses contributed to further deterioration of cardiac function, likely due to the increased presence of cytokine-expressing immune cells exacerbating myocardial damage.

Our study revealed the potential impact of IL-21 on myocardial fibrosis. We first found that IL-21R knockout significantly alleviated ISO-induced myocardial fibrosis (Fig. 3). Through co-culture experiments, we observed that Th1 cells from ISO-treated WT mice secreted increased levels of IFN- $\gamma$ , which in turn enhanced Th1 cell adhesion to cardiac fibroblasts (CFBs) and promoted the transformation of CFBs into myofibroblasts. To further confirm whether this adhesion effect was mediated by IFN- $\gamma$ , anti-IFN- $\gamma$  neutralizing antibodies were added into the co-culture system. Our results showed that blocking IFN- $\gamma$  significantly reduced the adhesion of Th1 cells to CFBs, supporting the role of IFN- $\gamma$  in this process (Fig. 4). This adhesion effect was mediated by IFN- $\gamma$  secreted by Th1 cells<sup>16</sup>. IL-21R knockout significantly reduced this transformation effect, suggesting that IL-21 may exacerbate myocardial fibrosis by enhancing Th1 cell function (Fig. 4). Other studies have also indicated that IL-21 not only affects the fibrotic process in the heart but may also influence the overall cardiac pathological environment by modulating the functions of other immune cell types<sup>20,21,27</sup>. Additionally, to evaluate the effect

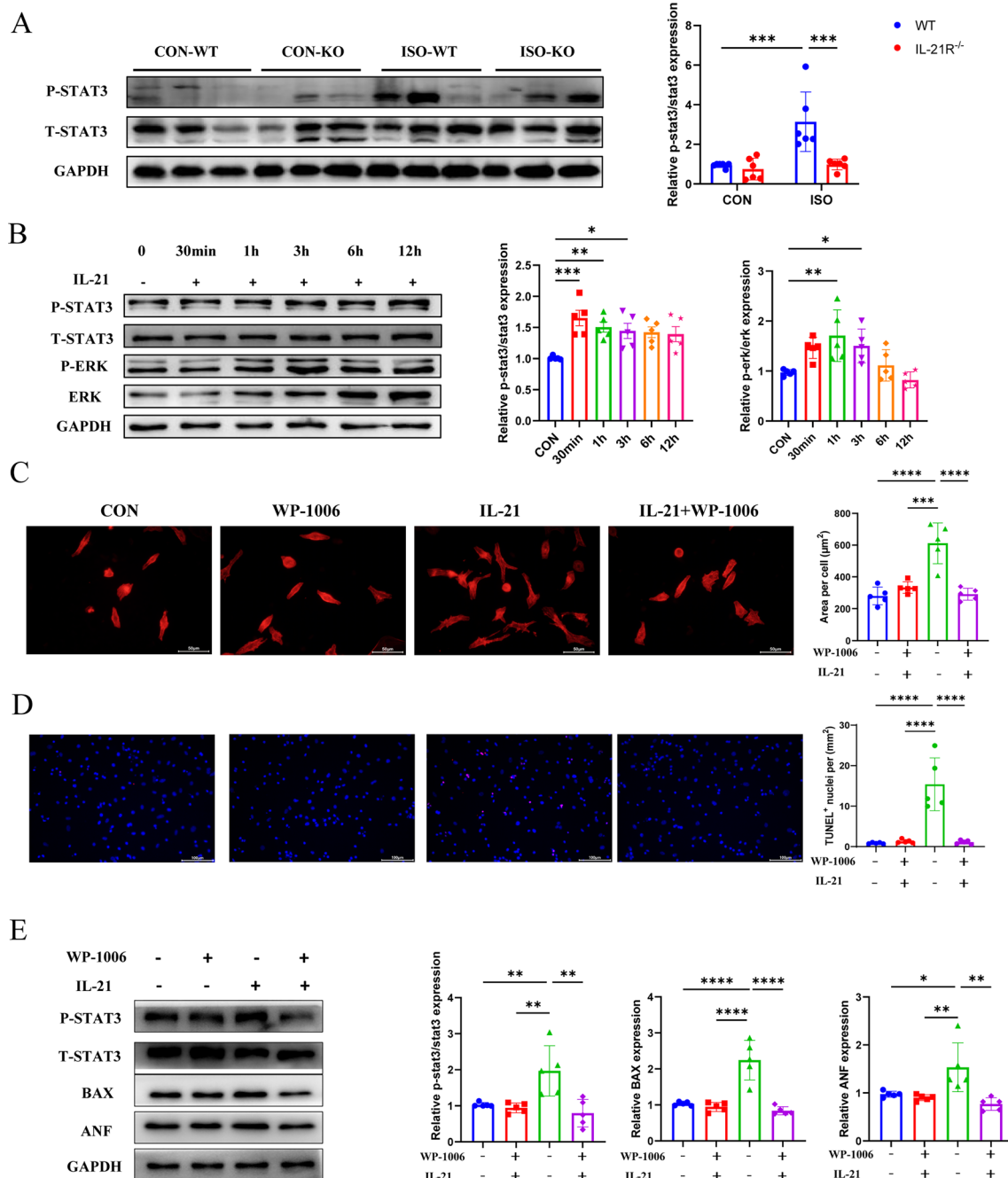


**Fig. 6.** IL-21 controls cardiomyocyte hypertrophy and apoptosis by activating the STAT3 pathway. Primary mouse cardiomyocytes were treated with IL-21 (100 ng/ml) and WP1006 (3  $\mu\text{mol/L}$ ) for 24 h for subsequent analyses. (A) Western blot analysis of phosphorylated STAT3 (p-STAT3) and total-STAT3 in myocardial tissue and their quantification,  $n = 6$ . (B) Western blot analysis of p-STAT3, total-STAT3, p-ERK and ERK expression in primary mouse cardiomyocytes after IL-21 treatment for different durations and their quantification,  $n = 5$ . (C) Representative phalloidin staining images of primary cardiomyocytes and quantification of cell area,  $n = 6$ , scale bar: 50  $\mu\text{m}$ . (D) Representative TUNEL staining of primary cardiomyocytes and quantification of TUNEL staining,  $n = 6$ , scale bar: 100  $\mu\text{m}$ . (E) Western blot analysis of p-STAT3, total-STAT3, ANF, and BAX expression in primary mouse cardiomyocytes after 24-h treatment with IL-21 and WP1006 and their quantification,  $n = 5$ . Data are presented as mean  $\pm$  SEM. \* $p < 0.05$ , \*\* $p < 0.01$ , \*\*\* $p < 0.001$ , \*\*\*\* $p < 0.0001$ .

of T cells on cardiomyocytes, we conducted a 24-h co-culture experiment using primary cardiomyocytes and isolated CD4<sup>+</sup> T cells (Fig. S5B,C). The results showed no significant differences in the adhesion of T cells to cardiomyocytes in different treatment groups. Furthermore, qPCR analysis indicated no notable changes in the expression of inflammatory or apoptotic markers, such as BAX and Bcl-2, in cardiomyocytes under these conditions. These findings suggest that, under a 24-h experimental setting, T cells may not have a significant

impact on cardiomyocyte inflammation or apoptosis. However, since cell–cell interactions may be time-dependent, further studies are needed to explore the potential effects of T cells on cardiomyocyte function over longer co-culture periods or under different experimental conditions.

We further explored the mechanisms by which IL-21 regulates cardiomyocyte hypertrophy and apoptosis through the STAT3 signaling pathway. IL-21R knockout attenuated ISO-induced cardiac hypertrophy and cardiac dysfunction, indicating that IL-21R plays a promotive role in ISO-induced pathological cardiac remodeling (Fig. 1 and 2). This finding is consistent with previous studies<sup>19,28</sup>, which have shown that IL-21 is involved in the development and progression of cardiovascular diseases by modulating immune responses and inflammatory processes. We also found that IL-21 can directly act on the myocardium, inducing both myocardial hypertrophy and apoptosis (Fig. 5). Our data also revealed the role of IL-21 in regulating myocardial hypertrophy and apoptosis via the STAT3 signaling pathway (Fig. 6). STAT3 is a well-known transcription factor that plays various roles in cell proliferation, differentiation, and survival<sup>29–31</sup>. In our experiments, IL-21 treatment significantly activated the STAT3 signaling pathway and upregulated the expression of hypertrophy-related genes ANF, BNP, and the pro-apoptotic protein BAX. Furthermore, by using the STAT3 inhibitor WP-1006, we found that IL-21-induced cardiomyocyte hypertrophy and apoptosis could be attenuated (Fig. 6). This result not only confirms the role of STAT3 in IL-21-mediated cardiac injury but also suggests that STAT3 could be a potential therapeutic target for treating myocardial hypertrophy and heart failure. Furtek et al. also highlighted the potential of STAT3 inhibitors in cancer therapy, which further supports the feasibility of targeting STAT3 in cardiovascular disease treatment<sup>32</sup>.

Additionally, to investigate whether IL-21 directly affects fibroblast activation and apoptosis, we stimulated primary cardiac fibroblasts with IL-21 and analyzed the expression of fibrosis- and apoptosis-related genes after 24 h. qPCR results showed no significant changes in the expression of TGF-β, α-SMA, Fn1, collagen I, collagen III, or collagen IV, and no notable changes in the expression of the pro-apoptotic gene BAX or the anti-apoptotic gene Bcl-2 (Fig. S5A). These findings suggest that, under a 24-h experimental condition, IL-21 may not directly induce fibroblast activation or apoptosis. However, this does not exclude the possibility of long-term effects or interactions with other cell types influencing the myocardial fibrosis process. Therefore, further studies are needed to explore the long-term role of IL-21 in myocardial fibrosis.

Existing evidence indicates that IL-21 and IL-21R play important roles in cardiac health and disease (Fig. 7), and their roles in heart health and disease have increasingly garnered attention. They are not only involved in the regulation of the immune system but may also directly affect the function of cardiac cells. Future research should focus on elucidating the specific mechanisms of the IL-21/IL-21R signaling pathway in cardiac diseases and exploring its potential as a therapeutic target.

## Material and methods

### Animal

Male C57BL/6 mice (18–22 g, 6–8 weeks old) were obtained from SPF Biotechnology. IL-21R<sup>-/-</sup> mice were purchased from Nanjing Biomedical Research Institute. These IL-21R<sup>-/-</sup> mice were viable, had normal phenotypes and no overt abnormalities. Mice were bred and maintained under specific pathogen-free (SPF) conditions. They were provided with normal food and water ad libitum and maintained in an air-conditioned room with a 12-h light/dark cycle. All animal experiments were approved by the Ethics Committee of Nankai University (Approval No: 10011) and performed in accordance with institutional guidelines. Isoproterenol (ISO) was administered subcutaneously in the dorsal region of the mice (30 mg/kg/day, Solarbio) for 7 days. One week after saline injection in the control group, echocardiographic analysis was performed 24 h following the final ISO injection using M-mode to assess left ventricular (LV) systolic function, including ejection fraction (EF), fractional shortening (FS), atrial natriuretic factor (ANF) expression, and the extent of interstitial fibrosis. During the ultrasound examination, the heart rate of the mice was approximately 400 beats per minute. Additionally, data on the end-diastolic left ventricular anterior and posterior wall dimensions have been included in Supplementary Table 2. This study was conducted in accordance with the ARRIVE guidelines and an ARRIVE study plan was prepared to ensure rigorous and ethical reporting of animal research.

### Echocardiographic evaluation

At the end of the study, echocardiography was performed. We used M-mode echocardiography with a 17.5 MHz liner array transducer system (Vevo 2100™ High Resolution Imaging System; Visual Sonics). Left ventricular function was assessed by measuring fractional shortening (FS), ejection fraction (EF), and heart rate. All measurements were performed by one researcher who was blind to the experimental groups. The animals were euthanized by intraperitoneal injection of an overdose of pentobarbital sodium (at a dosage of approximately 150 mg/kg).

### Primary mouse cardiomyocyte and fibroblast culture

Hearts from newborn mice (< 24 h old, SPF Biotechnology) were placed in ice-cold Hanks' balanced salt solution, minced into small pieces, and digested with trypsin for 7 h at 4 °C. The heart tissue fragments were then further digested with type II collagenase at 37 °C. The digested cardiomyocytes were collected by centrifugation at 500 g for 5 min. Cells were then subjected to two rounds of differential adhesion at 37 °C for 75 min each to isolate primary mouse cardiomyocytes and primary fibroblasts for subsequent co-culture experiments.

### Preparation of mononuclear cells

After the final subcutaneous injection of isoproterenol, mediastinal lymph nodes (mLNs) were collected and the cells were dispersed using a syringe plunger. The cell suspension was filtered through a 40 µm cell strainer, and the lymphocytes were washed and resuspended for subsequent experiments.

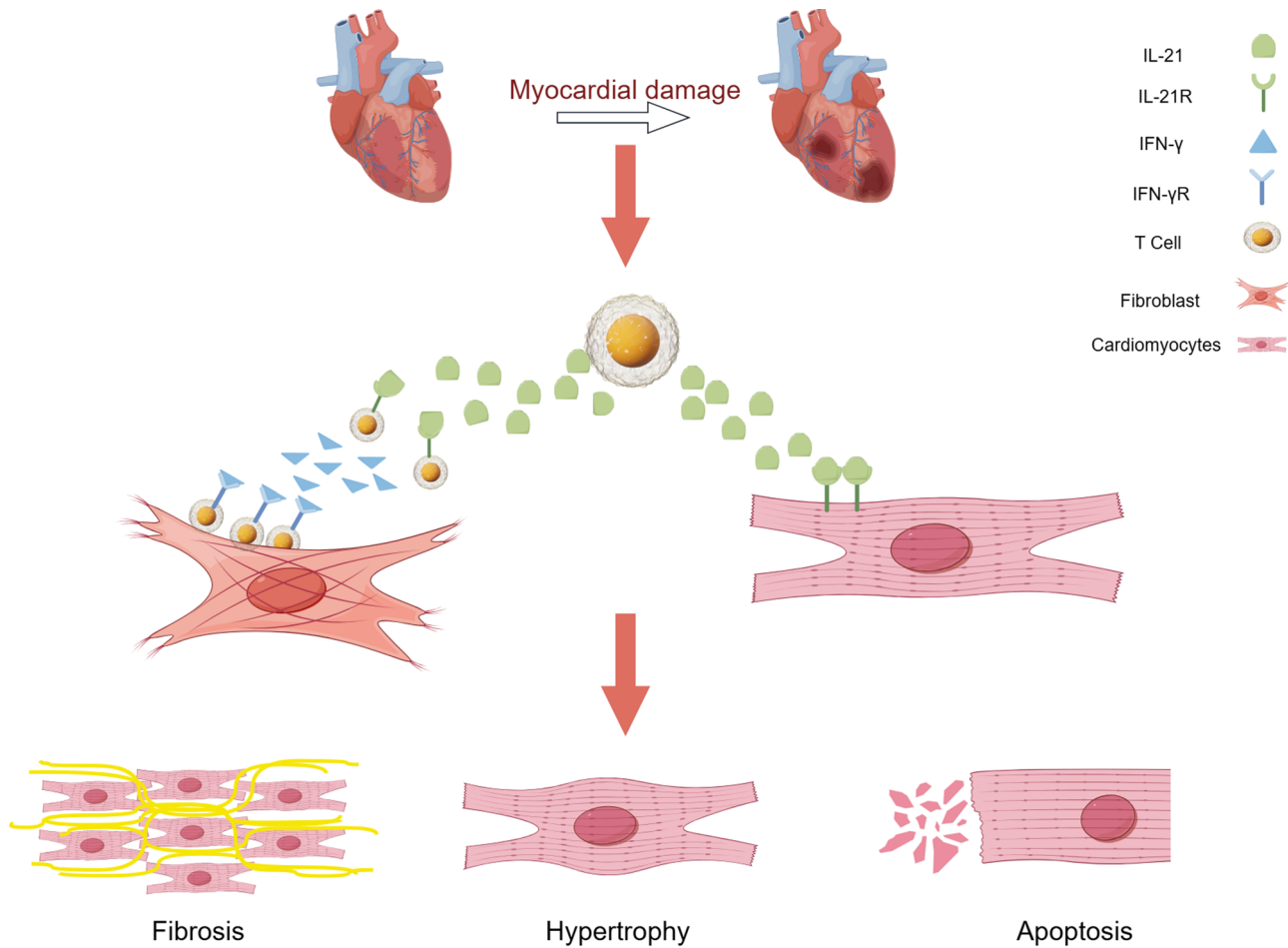


**Fig. 7.** Schematic representation of IL-21/IL21R-mediated cardiac remodeling in HF mice. Pressure overload induces upregulation of IL-21 and the IL-21 receptor in the myocardium. On the one hand, IL-21 promotes an increase in IFN- $\gamma$  secreting T cells, which subsequently increases the adhesion of T cells to fibroblasts, thereby aggravating myocardial fibrosis. On the other hand, IL-21 directly binds to IL21R on the surface of cardiomyocytes, which promotes gene expression and signal transduction related to cardiac hypertrophy and apoptosis, leading to these pathological changes. These two different processes combine to exacerbate myocardial injury in mice. This figure was created using Figdraw (URL: <https://www.figdraw.com/static/index.html#/l/>).

### Flow cytometry analysis

Immune cells from the mLNs were stained for 30 min at 4 °C with the following antibodies: FITC anti-mouse CD4 $^{+}$ , FITC anti-mouse Ly-6C $^{+}$ , FITC anti-mouse Ly6-G $^{+}$ , PE anti-mouse IL-21 $^{+}$ , and APC anti-mouse IFN- $\gamma$  $^{+}$ , (all from BioLegend). The stained cells were analyzed with a flow cytometer (Becton Dickinson). mLNs were used to isolate CD4 $^{+}$  T cells via flow cytometry-based cell sorting.

### Preparation of T cells and fibroblast co-culture in vitro

Seven days after subcutaneous injection of ISO, CD4 $^{+}$  T cells were isolated from the middle mediastinal lymph nodes (mLNs) of WT mice and IL-21R $^{-/-}$  mice by flow cytometric sorting and then immediately used for in vitro coculture experiments. Primary fibroblasts were seeded in 6-well plates. Then half of the culture medium was removed and the T cell suspension was added to each well. Furthermore, in the experimental group where CD4 $^{+}$  T cells from ISO-treated WT mice were co-cultured with CFBs, exogenous IFN- $\gamma$  antibody (Bioxcell) was additionally added. T cells and CFBs were co-cultured at 37 °C and 5% CO<sub>2</sub>. After 24 h, cells were washed with PBS. After washing, microscopic images were taken. After washing, cells were fixed for immunofluorescence staining.

### Histology

Cardiac tissue was fixed in 4% paraformaldehyde, followed by dehydration, clearing, and paraffin embedding. The heart tissue was then cut into 5  $\mu$ m thick samples for subsequent experiments. For immunohistochemical staining, tissue sections were baked at 65 °C for 2 h, deparaffinized, and rehydrated, followed by antigen retrieval in 0.01 M citrate buffer (Solarbio Biotechnology). The sections were blocked with 5% goat serum for 1 h and then incubated with IL-21 and IL-21R antibodies (both from Affinity) (1:200) overnight at 4 °C. After washing,

HRP-conjugated secondary antibodies were applied for 30 min at room temperature. Finally, the sections were counterstained with hematoxylin. According to standard procedures, sections were stained with hematoxylin and eosin (H&E) (Beyotime Biotechnology), Masson's trichrome (ZSGB-BIO), WGA (Sigma-Aldrich), Sirius Red (Solarbio Biotechnology), and TUNEL (Abbkine). To assess changes in cell morphology, treated cells were fixed, permeabilized, and incubated with phalloidin (Yeasen Biotechnology) for 30 min at 37 °C, and images were captured with a fluorescence microscope (Nikon, Tokyo, Japan).

### Immunofluorescence

Frozen heart sections or primary fibroblasts from co-culture were permeabilized after washing and fixing with 0.5% Triton X-100 at room temperature for 15 min and then blocked with 5% goat serum at room temperature for 1 h. Samples were treated overnight at 4 °C with cTnT (Invitrogen, 1:200), IL-21 (Affinity, 1:200), IL-21R (Affinity, 1:200), and α-SMA (Sigma, 1:200). After washing in TBST, samples were incubated with appropriate Alexa Fluor 488 or Alexa Fluor 594-conjugated secondary antibodies (ZSGB-BIO, 1:200) for 1 h at room temperature. Nuclei were stained with DAPI for 2 min at room temperature. The confocal microscope (Olympus FV1000) was used to capture high-resolution images.

### RT-PCR and quantitative real-time PCR (qPCR) assays

Total RNA was extracted from cardiac tissue and cells using Trizol reagent (Takara Biotechnology) according to the manufacturer's instructions. cDNA synthesis was performed using the reverse transcription system (TransGen Biotechnology). Real-time polymerase chain reaction (PCR) was performed using SYBR Green Master Mix (TransGen Biotechnology) on a Roche LightCycler 96 detection system. The sequences are listed in Supplementary Table 1. Relative quantification of target gene expression was normalized to the reference gene β-actin.

### Western blot analysis

Left ventricular tissue and cell samples were lysed in ice-cold RIPA lysis buffer and centrifuged at 12,000 g for 30 min at 4 °C. Total protein concentration was measured using a BCA protein assay kit (Thermo). Protein samples (20–50 µg) were separated by 10% and 12% SDS-PAGE and transferred to polyvinylidene difluoride (PVDF) membranes (Merck KGaA). Membranes were cropped prior to hybridization with antibodies. After blocking with 5% nonfat milk for 2 h, the membranes were incubated overnight at 4 °C with primary antibodies, including anti-IL-21 (Affinity), anti-p-STAT3 (Zenbio), anti-STAT3 (CST), anti-BAX (CST), anti-ANF (Proteintech), anti-α-SMA (Sigma), anti-Collagen I (ABclonal), and anti-GAPDH (Proteintech). The membranes were then incubated with HRP-conjugated secondary antibodies for one hour at room temperature. Target bands were detected using Sparkjade ECL Super (Sparkjade Biotechnology) and analyzed using ImageJ, with results expressed as fold changes normalized to GAPDH.

### Statistical analysis

The data presented in this study represent at least three independent experiments and are expressed as mean ± standard deviation (SD). All data is presented in the form of bar graphs. Statistical analysis was performed using GraphPad Prism 9. Statistical significance between two groups was determined using Student t test. One-way or two-way ANOVA was used for comparisons between multiple groups, followed by Tukey's or Dunnett's post hoc test for multiple comparisons between three or more groups. A P-value of < 0.05 was considered statistically significant.

### Data availability

All data generated or analyzed during this study are included in this published article [and its supplementary information files].

Received: 25 October 2024; Accepted: 14 May 2025

Published online: 30 May 2025

### References

- Ponikowski, P. et al. 2016 ESC Guidelines for the diagnosis and treatment of acute and chronic heart failure. *Kardiol. Pol.* **74**(10), 1037–1147 (2016).
- Bui, A. L., Horwitz, T. B. & Fonarow, G. C. Epidemiology and risk profile of heart failure. *Nat. Rev. Cardiol.* **8**(1), 30–41 (2011).
- Tanai, E. & Frantz, S. Pathophysiology of Heart Failure.
- Frangogiannis, N. G. Pathophysiology of myocardial infarction. *Compr. Physiol.* **5**(4), 1841–1875 (2015).
- Schiattarella, G. G. & Hill, J. A. Inhibition of hypertrophy is a good therapeutic strategy in ventricular pressure overload. *Circulation* **131**(16), 1435–1447 (2015).
- Westermann, D. et al. Cardiac inflammation contributes to changes in the extracellular matrix in patients with heart failure and normal ejection fraction. *Circ. Heart Fail.* **4**(1), 44–52 (2011).
- Liu, Z. et al. IL-21 enhances NK cell activation and cytolytic activity and induces Th17 cell differentiation in inflammatory bowel disease. *Inflamm. Bowel Dis.* **15**(8), 1133–1144 (2009).
- Davis, M. R. et al. The role of IL-21 in immunity and cancer. *Cancer Lett.* **358**(2), 107–114 (2015).
- Spolski, R. & Leonard, W. J. Interleukin-21: Basic biology and implications for cancer and autoimmunity. *Annu. Rev. Immunol.* **26**(1), 57–79. <https://doi.org/10.1146/annurev.immunol.26.021607.090316> (2008).
- Leonard, W. J. & Spolski, R. Interleukin-21: A modulator of lymphoid proliferation, apoptosis and differentiation. *Nat. Rev. Immunol.* **5**(9), 688–698 (2005).
- Zeng, R. et al. Synergy of IL-21 and IL-15 in regulating CD8+ T cell expansion and function. *J. Exp. Med.* **201**(1), 139–148 (2005).
- Spolski, R. & Leonard, W. J. Interleukin-21: A double-edged sword with therapeutic potential. *Nat. Rev. Drug Discov.* **13**(5), 379–395 (2014).

13. Caruso, R. et al. Involvement of interleukin-21 in the epidermal hyperplasia of psoriasis. *Nat. Med.* **15**(9), 1013–1015 (2009).
14. Weir, R. A. P. et al. Interleukin-21—a biomarker of importance in predicting myocardial function following acute infarction? *Cytokine* **60**(1), 220–225 (2012).
15. Xing, Y. et al. Targeting interleukin-21 inhibits stress overload-induced cardiac remodelling via the TIMP4/MMP9 signalling pathway. *Eur. J. Pharmacol.* **940**, 175482 (2023).
16. Nevers, T. et al. Th1 effector T cells selectively orchestrate cardiac fibrosis in nonischemic heart failure. *J. Exp. Med.* **214**(11), 3311–3329 (2017).
17. Davis, I. D. et al. Interleukin-21 signaling: Functions in cancer and autoimmunity. *Clin. Cancer Res.* **13**(23), 6926–6932 (2007).
18. Ding, R. et al. Effect of serum interleukin 21 on the development of coronary artery disease. *APMIS* **122**(9), 842–847 (2014).
19. Kubota, A. et al. Inhibition of Interleukin-21 prolongs the survival through the promotion of wound healing after myocardial infarction. *J. Mol. Cell Cardiol.* **159**, 48–61 (2021).
20. Hara, A. & Tallquist, M. D. Fibroblast and immune cell cross-talk in cardiac fibrosis. *Curr. Cardiol. Rep.* **25**(6), 485–493 (2023).
21. Zambrano, M. A. & Alcaide, P. Immune cells in cardiac injury repair and remodeling. *Curr. Cardiol. Rep.* **25**(5), 315–323 (2023).
22. Perticone, M. et al. Immunity, inflammation and heart failure: Their role on cardiac function and iron status. *Front. Immunol.* **10**, 2315 (2019).
23. Li, H., Chen, C. & Wang, D. W. Inflammatory cytokines, immune cells, and organ interactions in heart failure. *Front. Physiol.* <https://doi.org/10.3389/fphys.2021.695047> (2021).
24. Cohen, C. D. et al. Myocardial immune cells: The basis of cardiac immunology. *J. Immunol.* **210**(9), 1198–1207 (2023).
25. Bengel, F. et al. Linking immune modulation to cardiac fibrosis. *Nat. Cardiovasc. Res.* **3**(4), 414–419 (2024).
26. Baci, D. et al. Innate immunity effector cells as inflammatory drivers of cardiac fibrosis. *Int. J. Mol. Sci.* **21**(19), 7165 (2020).
27. Liberale, L. et al. Cytokines as therapeutic targets for cardio- and cerebrovascular diseases. *Basic Res. Cardiol.* **116**(1), 23 (2021).
28. Xing, Y. et al. Targeting interleukin-21 inhibits stress overload-induced cardiac remodelling via the TIMP4/MMP9 signalling pathway. *Eur. J. Pharmacol.* **940**, 175482 (2023).
29. Yu, H. et al. Revisiting STAT3 signalling in cancer: New and unexpected biological functions. *Nat. Rev. Cancer* **14**(11), 736–746 (2014).
30. Demaria, M. et al. Cellular senescence promotes adverse effects of chemotherapy and cancer relapse. *Cancer Discov.* **7**(2), 165–176 (2017).
31. Zou, S. et al. Targeting STAT3 in cancer immunotherapy. *Mol. Cancer* **19**(1), 145 (2020).
32. Furtek, S. L. et al. Strategies and approaches of targeting STAT3 for cancer treatment. *ACS Chem. Biol.* **11**(2), 308–318 (2016).

## Author contributions

B.Q: Conceptualization, Methodology, Validation, Formal analysis, Investigation, Writing - Original Draft, Visualization. R.X, Y.J, Y.W, T.C, C.L, Y.j: Validation, Formal analysis, Investigation, Visualization. L.G, J.L, Y.G, J.L, Y.X, J.C: Formal analysis, Resources, Supervision, Project administration. Z.J, L.F, Z.Q and L.Y: Resources, Writing - Review & Editing, Project administration, Funding acquisition.

## Funding

This work was supported by the National Natural Science Foundation of China (Nos. 32271327, 82372195, 82172170, 32071263, 82072187 and 32301071); China Postdoctoral Science Foundation (No. 2023M731807). Tianjin Natural Science Foundation (23JCQNJC01820). NanKai University Eye Institute (NKYKK202201).

## Declarations

### Competing interests

The authors declare no competing interests.

### Additional information

**Supplementary Information** The online version contains supplementary material available at <https://doi.org/10.1038/s41598-025-02552-4>.

**Correspondence** and requests for materials should be addressed to Z.J., L.F., Z.Q. or L.Y.

**Reprints and permissions information** is available at [www.nature.com/reprints](http://www.nature.com/reprints).

**Publisher's note** Springer Nature remains neutral with regard to jurisdictional claims in published maps and institutional affiliations.

**Open Access** This article is licensed under a Creative Commons Attribution-NonCommercial-NoDerivatives 4.0 International License, which permits any non-commercial use, sharing, distribution and reproduction in any medium or format, as long as you give appropriate credit to the original author(s) and the source, provide a link to the Creative Commons licence, and indicate if you modified the licensed material. You do not have permission under this licence to share adapted material derived from this article or parts of it. The images or other third party material in this article are included in the article's Creative Commons licence, unless indicated otherwise in a credit line to the material. If material is not included in the article's Creative Commons licence and your intended use is not permitted by statutory regulation or exceeds the permitted use, you will need to obtain permission directly from the copyright holder. To view a copy of this licence, visit <http://creativecommons.org/licenses/by-nc-nd/4.0/>.

© The Author(s) 2025